Excitons on the surface of a sphere

Thomas G. Pedersen
Department of Physics and Nanotechnology, Aalborg University, DK-9220 Aalborg Øst, Denmark
(Received 21 October 2009; revised manuscript received 16 March 2010; published 24 June 2010)

Low-dimensional excitons are normally modeled as electron-hole pairs confined to a restricted volume. In certain cases, however, confinement to a restricted surface is a more appropriate model. These cases include one-dimensional carbon nanotubes but also various zero-dimensional structures such as small oxidized Si nanoparticles and spherical core/well/shell quantum dots. Wannier excitons confined to spherical surface quantum wells of finite and zero thicknesses are analyzed using numerical, analytical, and variational methods. The results are applied to known zero-dimensional structures supporting surface-confined excitons.

DOI: 10.1103/PhysRevB.81.233406 PACS number(s): 71.35.−y, 78.67.Bf

Excitons play an important role in the optical properties of semiconductor nanostructures.[1,2] Primarily, quantum confinement leads to increased electron-hole overlap, thereby enhancing the exciton binding energy to values comparable to or above room-temperature thermal energies. For perfect confinement in a quantum well (two-dimensional limit), the binding energy of the lowest Wannier exciton measured in effective Rydbergs Ry^* increases to $E=-4Ry^*$, which is precisely a factor of four larger than the bulk value.[3] For quasi-one-dimensional quantum wires and zero-dimensional quantum dots the effect may be even more pronounced.[4,5] Such low-dimensional excitons may be modeled as interacting electrons and holes confined to a restricted volume in space by means of barriers formed by band offsets between different materials. In certain cases, however, a picture of electron-hole pairs confined to the surface of a nanostructure is more appropriate. The classical example is that of a carbon nanotube, for which excitons are confined to a cylindrical surface.[6,7]

Surface-confined excitons exist in zero-dimensional nanostructures as well. Hence, these states can be viewed as interacting electron-hole pairs living on the surface of a sphere. Physical realizations of such structures include oxidized Si and Ge nanodots,[8,9] spherical core/well/shell nanoparticles[10] and, to some extent, C_{60} and other fullerenes. The confinement mechanism differs among these cases. For Si nanodots, band gap lowering by partial oxidation[11] is believed to be responsible.[8] In CdS/CdSe/CdS core/well/shell structures, band offsets between CdS and CdSe lead to confinement in a spherical quantum well. Finally, electrons and holes are confined to the carbon atom π-orbital network in fullerenes similarly to the case of carbon nanotubes. In the present work, a simple description of excitons confined to spherical surfaces is formulated and analyzed. The model is restricted to Wannier-type excitons in that we adopt the effective-mass approximation, treat the Coulomb interaction in the Hartree approximation and ignore exchange effects. We consider both (i) perfect confinement in an infinitely thin radial quantum wells as well as (ii) confinement by a radial potential of finite width. The simplicity of the first case is appealing from a conceptional point of view. Moreover, a cylindrical model based on similar assumptions is known to successfully reproduce the measured structure dependence of exciton resonances in carbon nanotubes[12] and agrees with the scaling behavior found in the highly advanced Bethe-Salpeter approach.[13] Finally, the limit of perfect radial confinement with vanishing well thickness can be compared to recent work on the problem of two electrons on a spherical surface.[14–16] We will demonstrate that analytical solutions for higher (positive-energy) exciton states can be found for certain nanoparticle radii using the recursive method of Ref. 16. In addition, a highly accurate variational estimate can be given for the ground state. The general theory is applied to the physical realizations mentioned above in order to provide estimates of binding energies of surface excitons in various spherical nanostructures. We stress, however, that accuracy of the model is not expected to compete with advanced *ab initio* results. Rather, the strength lies is its conceptual simplicity and greatly reduced computational cost. The analytical solutions found below are valuable additions to the very short list[1,2] of exactly solvable exciton models. Finally, the present model could be extended to multiparticle complexes with only a modest computational demand.

The geometry used to describe exciton states is sketched in the inset of Fig. 1. The radius R is the average between inner and outer radii of the spherical quantum well and d is the width of the well. The angular separation between electron and hole is θ and the distance u is therefore $u=R\sqrt{2(1-\cos\theta)}$. In reality, electrons and holes are smeared out in the radial range between $R-d/2$ and $R+d/2$. Thus, the effective Coulomb interaction is reduced from the simple u^{-1} point-particle behavior, in particular, for small angular separation. To model the effective Coulomb attraction we assume that the thickness d of the spherical quantum well is much smaller than the radius R. In this case, the radial parts of electron and hole wave functions can be approximately regarded as "frozen" in the lowest radial eigenstate. This approximation amounts to ignoring the influence of Coulomb forces on the radial motion. If these radial eigenstates are denoted $\phi_e(r)$ and $\phi_h(r)$ for electrons and holes, respectively, it follows that the effective interaction between the particles is $-2V_{eff}$ with

$$V_{eff}(\theta)=\int_0^\infty\int_0^\infty \frac{|\phi_e(r_e)|^2|\phi_h(r_h)|^2}{\sqrt{r_e^2+r_h^2-2r_er_h\cos\theta}}r_e^2r_h^2dr_edr_h. \quad (1)$$

Only $l=0$ radial states pertaining to vanishing single-particle angular momentum are considered. Moreover, we assume that the radial confinement resembles a parabolic well and, thereby, that the radial eigenstates can be approximated by identical Gaussians $\phi_e(r)=\phi_h(r)=N\exp[-(r-R)^2/d^2]$,

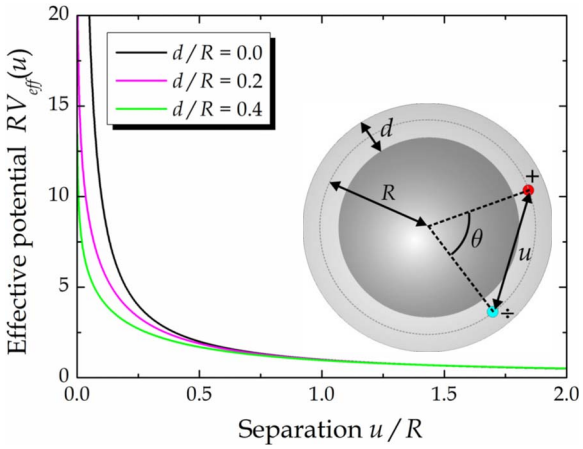

FIG. 1. (Color online) Effective Coulomb interaction for different thicknesses of the confining quantum well. The geometrical parameters for an electron-hole pair confined to the well are shown in the inset.

where N is a normalization constant. If polar coordinates $r_e = \rho \cos \eta$ and $r_h = \rho \sin \eta$ are introduced the integral above reduces to

$$V_{eff}(\theta) = \int_0^{\pi/2} \frac{F(\eta)}{\sqrt{1 - \sin 2\eta \cos \theta}} d\eta, \tag{2}$$

where

$$F(\eta) = N^4 \int_0^{\infty} \exp\{-[2\rho^2 + 4R^2 - 4\rho R(\cos \eta + \sin \eta)]/d^2\} \times \rho^4 d\rho \approx \sqrt{\frac{2}{\pi}} \frac{4}{d} e^{2R^2/d^2(\sin 2\eta - 1)}. \tag{3}$$

Using elementary integrals[17] and introducing the parameter $z = R^2(\sec \theta - 1)/2d^2 = u^2/(4d^2 - 2u^2d^2/R^2)$ allows us to express the final result in the compact form

$$V_{eff}(u) = \frac{1}{u} \sqrt{\frac{2z}{\pi}} e^z K_0(z). \tag{4}$$

Hence, the factor $\sqrt{2z/\pi} e^z K_0(z)$ is a measure of the deviation from simple u^{-1} behavior. Strictly speaking, Eq. (4) acquires a small imaginary part whenever $z < 0$ that should obviously be excluded in actual calculations. Hence, only the real part of V_{eff} is retained if $z < 0$. From the asymptotic behaviors of the Bessel function K_0 it is readily shown that for fixed distance u the limiting behavior for a thin quantum well is $\lim_{d \to 0} V_{eff}(u) = u^{-1}$ as required and similarly for $u \ll d, R$ (with Euler's constant $\gamma = 0.57721\ldots$)

$$V_{eff}(u) \approx -\frac{\gamma + 2 \ln\left(\frac{u}{d\sqrt{8}}\right)}{d\sqrt{2\pi}}, \tag{5}$$

so that the divergence is logarithmic and independent of R for small electron-hole separations.

In analogy with the two-electron problem,[14–16] the Wannier equation for the exciton wave function ψ describes the relative motion of the electron-hole pair in terms of the polar angle θ and an azimuth angle ϕ. If u is substituted for θ, the equation reduces to the form

$$\left[\frac{u^2}{4R^2} - 1\right] \frac{d^2\psi}{du^2} + \left[\frac{3u}{4R^2} - \frac{1}{u}\right] \frac{d\psi}{du} - \frac{4R^2}{u^2(4R^2 - u^2)} \frac{d^2\psi}{d\phi^2} - 2V_{eff}(u)\psi = E\psi. \tag{6}$$

In this expression, all energies and distances are measured in units of effective Rydbergs Ry^* and Bohr radii a_B^*, respectively. Hence, the dependence on material parameters such as dielectric screening ε and effective reduced electron-hole pair mass μ (in units of the free-electron mass) enters via these quantities ($a_B^* = 0.529\ \text{Å} \cdot \varepsilon/\mu$ and $Ry^* = 13.6\ \text{eV} \cdot \mu/\varepsilon^2$) and must be considered when converting into physical units as detailed below. It is clear that the azimuthal dependence is of the simple form $\psi \propto e^{im\phi}$ with the angular momentum m an integer. Also, for numerical purposes, it is advantageous to introduce the scaled distance $x = u/2R$, $x \in [0,1]$. If we therefore write the wave function in the form $\psi = e^{im\phi} x^m (1 - x^2)^{m/2} \varphi(x)$ it can be shown that the one-dimensional Wannier equation for φ reads as

$$[x^2 - 1] \frac{d^2\varphi}{dx^2} + \left[(3 + 4m)x - \frac{1 + 2m}{x}\right] \frac{d\varphi}{dx} - 2v_{eff}(x)\varphi = [\varepsilon - 4m(m + 1)]\varphi, \tag{7}$$

where $\varepsilon = 4R^2E$ is the scaled energy and the scaled potential is

$$v_{eff}(x) = \frac{4R}{\delta\sqrt{2\pi(1 - 2x^2)}} \exp\left(\frac{x^2}{\delta^2(1 - 2x^2)}\right) K_0\left(\frac{x^2}{\delta^2(1 - 2x^2)}\right) \tag{8}$$

with $\delta = d/R$. In Fig. 1, the effective potential is shown for some illustrative examples ranging from perfect radial confinement ($\delta = 0$) to weak confinement ($\delta = 0.4$). The reduced effective interaction as radial confinement is weakened is clearly seen. Also, the logarithmic singularity can be perceived for cases of finite well thickness.

We solve Eq. (7) using a Jacobi polynomial basis[15] with basis functions of the form $\Phi_p(x) = \sqrt{2(p+1)} P_p^{(1,0)}(1 - 2x)$ with p a non-negative integer. These functions are orthonormal, i.e., $\int_0^1 \Phi_p(x)\Phi_q(x)xdx = \delta_{pq}$. The kinetic-energy matrix elements can be evaluated analytically whereas the matrix elements of Eq. (8) must be computed numerically. A method based on Gaussian quadrature with 1000 sample points is applied for this purpose. In addition, only the 25 lowest basis functions are included in the expansion. Note that for $m \neq 0$ the problem is not Hermetian. Results for the S-exciton ($m = 0$) binding energy E as a function of radius R are illustrated in Fig. 2. In each curve, d/R is fixed at a constant value so that the well thickness d constitutes a constant fraction of R. For $d/R = 0$, the asymptotic result for large spheres is $E = -4Ry^*$ in agreement with the result for excitons in two-dimensional quantum wells.[3] For $d/R \neq 0$, the binding energy keeps increasing toward zero with radius as the radial confinement of the exciton becomes gradually weaker. For large d, the approximation of a frozen radial wave function is

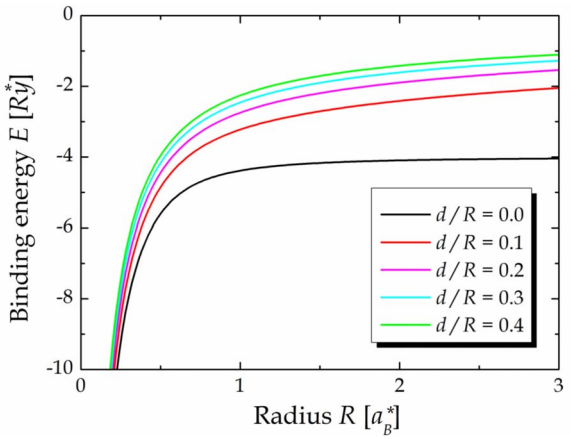

FIG. 2. (Color online) S-exciton binding energies vs radius for spherical quantum wells of varying thickness. As the radius decreases, a large enhancement of the binding energy is observed.

clearly inaccurate and, as a consequence, the large R limit differs from the exact limit $E=-1Ry^*$ found for a homogenous three-dimensional semiconductor. For $R<0.5a_B^*$, a substantial enhancement of the binding energy is observed regardless of the value of δ.

In the case of perfect radial confinement, i.e., $V_{eff}(u)=u^{-1}$, analytical solutions for the "unbound" states, that is, states with $E>0$ can be found for special values of the radius following the recursive approach of Loos and Gill.[16] Their work was applied to two electrons on a (hyper)spherical surface. Adopting the recursive approach to the electron-hole pair problem and writing $\varphi(x)=\Sigma_k s_k x^k$ with starting condition $s_1=-4Rs_0/(1+2m)$ leads to the expression

$$s_{k+2}=\frac{-4Rs_{k+1}+[k(k+4m+2)+4m(m+1)-4R^2E]s_k}{(k+2)(k+2m+2)}. \quad (9)$$

The polynomial series for $\varphi(x)$ terminates at a finite power x^p provided $s_{p+1}=s_{p+2}=0$. This condition provides a set of equations that can be solved simultaneously if E as well as R are both regarded as unknowns. For S excitons, the lowest radius for which such a solution is found is $R=\sqrt{3}/4$ with, correspondingly, $E=4$.

As the recursive method only applies to states with positive energy, it obviously cannot provide the lowest, ground-state, solution. However, a simple variational approach with an exponential ansatz for the wave function yields highly accurate results. Hence, writing $\varphi(x)\propto\exp(-\alpha x)$ it is readily demonstrated that the expectation value for the S-exciton energy is

$$E=\frac{3+6\alpha+4\alpha^2+16\alpha R+e^{2\alpha}(2\alpha^2-16\alpha R-3)}{8R^2(e^{2\alpha}-1-2\alpha)}. \quad (10)$$

Similar, but slightly more complicated expressions can be found for nonzero values of m. Minimizing with respect to α immediately provides the energy as well as the wave function. In Fig. 3, numerical solutions for S-type and P-type excitons ($m=0$ or 1, respectively) based on expansion in the Jacobi basis are compared to exact recursive solutions as well as the variational estimate of the lowest state. The

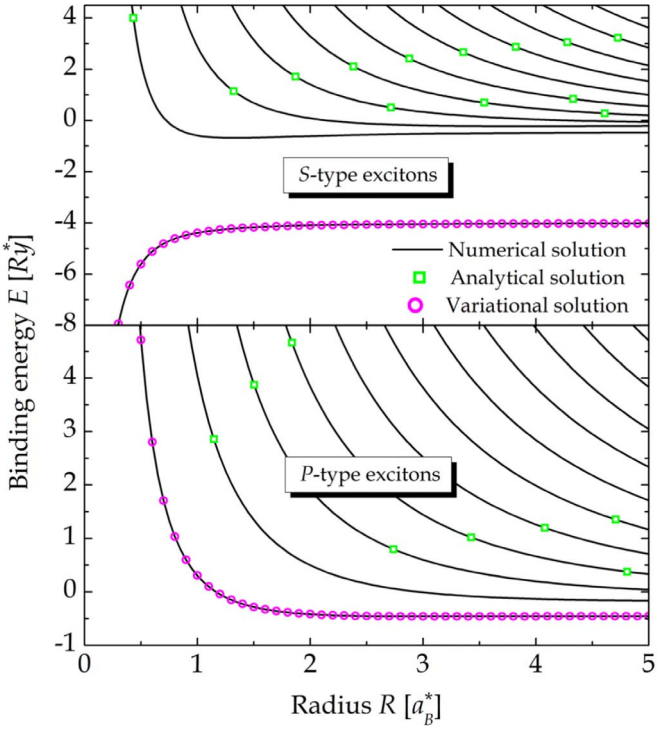

FIG. 3. (Color online) Binding energies for ideal radial confinement $d=0$ for S-type (upper panel) and P-type (lower panel) excitons. Numerical solutions (solid lines) are compared to analytical values (green squares) and variational estimates (magenta circles).

agreement between different methods is clearly excellent in all cases and, in fact, deviations cannot be discerned on the scale of the figure. The agreement between numerical and exact solutions testifies to the high accuracy of the basis expansion. Similarly, the agreement between numerical and variational methods implies a high degree of accuracy of the exponential ansatz.

Next, we turn to applications of the present theory. Specifically, we need to determine Ry^* and a_B^* for relevant spherical nanostructures, in addition to the geometric parameters R and d. As mentioned above, the candidates include (i) oxidized Si nanoparticles, (ii) spherical CdS(core)/CdSe(well)/CdS(shell) structures, and (iii) C_{60} molecules. We recall that R, as defined here, includes half the well thickness. In case (i), the mean radius for which excitons are confined in the surface well is $R\approx 3.5$ nm.[8] In addition, the well thickness is approximated by the lattice constant $d\approx 0.8$ nm of luminescent low-gap SiO.[18] For lack of a better value, we estimate the effective exciton Bohr radius of the interfacial layer by the Si value $a_B^*\approx 4.9$ nm (Ref. 19) and, moreover, assume that screening can be described by the average between Si and SiO_2 dielectric constants of 11.9 and 3.9, respectively, so that the resulting value is 7.9. These parameters correspond to an exciton Rydberg of 18.5 meV. For a two-monolayer CdSe well layer, case (ii) yields $R\approx 2.2$ nm and $d\approx 0.7$ nm.[10] Furthermore, for CdSe $Ry^*\approx 15$ meV,[20] which corresponds to $a_B^*\approx 5.2$ nm assuming a dielectric constant of 9.3. The case (iii) of C_{60} is obviously more delicate and it is doubtful if the present (solid-state) theory applies to such molecular species. Nevertheless,

TABLE I. Geometric parameters, natural exciton units and calculated *S*-exciton binding energies for three structures with surface-confined excitons.

Structure	R (nm)	d (nm)	Ry^* (meV)	a_B^* (nm)	E (Ry^*)	E (meV)
$Si/SiO/SiO_2$	3.5	0.8	18.5	4.9	−3.3	−61
CdS/CdSe/CdS	2.2	0.7	15.0	5.2	−4.8	−72
C_{60}	0.35	0.1	81	2.0	−10.8	−875

the successful application of similar theories to carbon nanotubes[6,12] indicates that, at least, rough agreement with experiments can be expected. The molecular radius defined as the distance between center and carbon nuclei is 0.35 nm and d can be estimated as roughly two (atomic) Bohr radii or 0.1 nm. The quasiparticle electronic energy gap of nearly isolated C_{60} is about 2.75 eV (Ref. 21) and modeling the molecule as a "graphene sphere" a band gap of this magnitude corresponds to an effective electron-hole pair mass of ~ 0.12 in units of the free-electron mass.[22] Also, the short-range graphene dielectric constant of 4.5 (Ref. 23) may be applied for crystalline C_{60} indicating that $Ry^* \approx 81$ meV and $a_B^* \approx 2.0$ nm. The geometric parameters of all structures are summarized in Table I along with the applied values of Ry^* and a_B^*. The table also includes computed *S*-exciton binding energies in Ry^* as well as millielectron volt. Notably, all *S*-exciton binding energies are above room-temperature thermal energies implying stability without sample cooling. Moreover, the energies clearly increase dramatically with decreasing particle size as expected from Figs. 2 and 3 even though differences in material parameters are taken into account. The finding that surface excitons are stable at room temperature in $Si/SiO/SiO_2$ and CdS/CdSe/CdS structures agrees with measurements of the temperature-dependent luminescence.[8,10] The computed values of the exciton binding energies cannot be directly compared to experiments, however. For C_{60}, the calculated binding energy of −875 meV is in practically perfect agreement with the highly advanced Bethe-Salpeter plus GW calculation for semi-isolated molecules by Tiago and Reboredo.[21] At an expanded lattice parameter of 14.8 Å for crystalline C_{60}, these authors find electronic and optical energy gaps of 2.75 eV and 1.85 eV, respectively, and thus an energy difference of −0.9 eV. The level of agreement is obviously partly fortuitous given the severe simplifications of the present theory and the uncertainty of the applied parameters. Nevertheless, it is gratifying that such a simple theoretical framework appears to have a wide applicability. We note that the binding energy for truly isolated C_{60} in vacuum is substantially larger[24] but the present solid-state model is clearly not suitable for such systems lacking bulk screening.

In summary, a simple model for excitons confined to a quantum well on a spherical surface has been developed. It provides estimates of binding energies and wave functions with greatly reduced computational cost compared to *ab initio* methods but naturally also with reduced reliability. Wells of finite thickness are allowed for through an effective electron-hole Coulomb interaction. Exciton binding energies are investigated numerically in the general case. The model simplifies substantially in the case of perfect radial confinement and here numerical results are shown to compare favorably with analytical solutions found for special nanoparticle radii as well as variational estimates. Finally, the theory is applied to a few semiconductor and molecular candidate structures and in all cases stable surface-confined excitons at room temperature are predicted in agreement with experiments.

Financial support from FTP under Grant No. 274-07-0523 project SERBINA is gratefully acknowledged.

[1] H. Haug and S. W. Koch, *Quantum Theory of the Optical and Electronic Properties of Semiconductors* (World Scientific, Singapore, 1993).
[2] P. K. Basu, *Theory of Optical Processes in Semiconductors* (Oxford Science, Oxford, 1997).
[3] M. Shinada and S. Sugano, J. Phys. Soc. Jpn. **21**, 1936 (1966).
[4] D. B. Tran Thoai *et al.*, Phys. Rev. B **42**, 11261 (1990).
[5] T. Ogawa and T. Takagahara, Phys. Rev. B **44**, 8138 (1991).
[6] T. G. Pedersen, Phys. Rev. B **67**, 073401 (2003).
[7] T. G. Pedersen *et al.*, Nano Lett. **5**, 291 (2005).
[8] Y. Kanemitsu *et al.*, Phys. Rev. B **48**, 4883 (1993).
[9] Y. Kanemitsu *et al.*, J. Lumin. **60-61**, 337 (1994).
[10] J. Xu *et al.*, Appl. Phys. Lett. **87**, 043107 (2005).
[11] P. Deák *et al.*, Phys. Rev. Lett. **69**, 2531 (1992).
[12] T. G. Pedersen, Carbon **42**, 1007 (2004).
[13] V. Perebeinos *et al.*, Phys. Rev. Lett. **92**, 257402 (2004).
[14] M. Seidl, Phys. Rev. A **75**, 062506 (2007).
[15] F. Loos and P. M. W. Gill, Phys. Rev. A **79**, 062517 (2009).
[16] F. Loos and P. M. W. Gill, Phys. Rev. Lett. **103**, 123008 (2009).
[17] I. S. Gradsteyn and I. M. Ryzhik, *Table of Integrals, Series and Products* (Academic Press, San Diego, 1994).
[18] Z. Hajnal *et al.*, Solid State Commun. **108**, 93 (1998).
[19] A. D. Yoffe, Adv. Phys. **50**, 1 (2001).
[20] P. Y. Yu and M. Cardona, *Fundamentals of Semiconductors* (Springer, Berlin, 2005).
[21] M. L. Tiago and F. A. Reboredo, Phys. Rev. B **79**, 195410 (2009).
[22] T. G. Pedersen *et al.*, Phys. Rev. B **79**, 113406 (2009).
[23] T. Ando, J. Phys. Soc. Jpn. **75**, 074716 (2006).
[24] M. L. Tiago *et al.*, J. Chem. Phys. **129**, 084311 (2008).